Bimetallic Zwitterionic Complexes with an Ambident Stanna-*closo*-dodecaborate Ligand: [1-{M(CO)$_5$}-2,7,8-(μ-H)$_3$-{Fe(triphos)}-SnB$_{11}$H$_{11}$] (M = Cr, Mo, W)

Torben Gädt, Klaus Eichele, and Lars Wesemann*

Institut für Anorganische Chemie der Universität Tübingen, Auf der Morgenstelle 18, Tübingen, D-72076, Germany

Received April 13, 2006

Starting from $FeBr_2$ the zwitterionic stannaborate complex [1-{Fe(MeCN)$_2$(triphos)}-SnB$_{11}$H$_{11}$] (**1**) could be obtained in a straightforward one-pot synthesis. Via a facile η^1(Sn) to η^3(BH) rearrangement reaction **1** can be converted into [2,7,8-(μ-H)$_3$-{Fe(triphos)}-SnB$_{11}$H$_{11}$] (**2**). The nucleophilicity of the tin atom in compound **2** is strongly reduced compared to the dianionic parent stannaborate cluster [SnB$_{11}$H$_{11}$]$^{2-}$. Methylation at the tin atom using standard methods is not feasible. Transition metal fragments can be coordinated at the tin atom of **2** if reactive species such as M(CO)$_5$(THF) (M = Cr, Mo, W) are employed. Reaction of these fragments with **2** yields the bimetallic zwitterions [1-{M(CO)$_5$}-2,7,8-(μ-H)$_3$-{Fe(triphos)}-SnB$_{11}$H$_{11}$] (M = Cr, Mo, W) (**3**, **4**, **5**), which contain an ambident stannaborate moiety. All new compounds have been characterized using ^{1}H, ^{11}B, ^{13}C, ^{31}P, and ^{119}Sn NMR spectroscopy as well as ^{31}P and ^{119}Sn MAS NMR experiments. Single-crystal X-ray diffraction analyses have been carried out for all novel compounds.

Introduction

There is ongoing interest in the chemistry of monocarbadodecaborate [CB$_{11}$H$_{12}$]$^-$ and its derivatives, which have been shown to behave as weakly coordinating anions[1] because of their very low basicity, polarizability, and high chemical stability. The growing interest in substituted derivatives of *closo*-boranes and carbaboranes is connected with the search for the least-coordinating derivative of [CB$_{11}$H$_{12}$]$^-$ [2] and has also stimulated work directed toward the understanding of substituent effects in this class of compounds.[3]

The monostannadodecaborate [SnB$_{11}$H$_{11}$]$^{2-}$ is a heavier homologue of the deprotonated borate [CB$_{11}$H$_{11}$]$^{2-}$. The nucleophilicity of the stannaborate at the tin atom has been described by the group of Todd, who showed that [SnB$_{11}$H$_{11}$]$^{2-}$ can be methylated with methyliodide to yield [1-CH$_3$-SnB$_{11}$H$_{11}$]$^-$.[4] This is in contrast to the electrophilicity of stannacarbaboranes such as [2,3-Me-1-Sn-2,3-C$_2$B$_9$H$_9$] and derivatives of 1-Sn-2,3-C$_2$B$_4$H$_6$ and 1-Sn-2,4-C$_2$B$_4$H$_6$, which are readily coordinated by Lewis bases such as 2,2′-bipyridine at the tin vertex.[5] On the other hand, stanna-*closo*-dodecaborate [SnB$_{11}$H$_{11}$]$^{2-}$ does not show electrophilicity but reacts as a nucleophile with alkyl halides and transition metal halides. The synthesis of the pentaanionic square planar gold complex [Au(SnB$_{11}$H$_{11}$)$_4$]$^{5-}$ from $AuCl_3$ and [Bu$_3$MeN]$_2$[SnB$_{11}$H$_{11}$] is a striking example.[6] As a general trend, the heteroborate coordinates at late transition metal fragments via tin−metal bonds. The remarkable variety of the tin−metal coordination modes with different gold fragments is exemplified by the μ_2 coordination in the dimeric complex [Au$_2$(SnB$_{11}$H$_{11}$)$_2$(PPh$_3$)$_2$]$^{2-}$, the μ_3 coordination in the triangular complex [{(Et$_3$P)Au(SnB$_{11}$H$_{11}$)}$_3$]$^{3-}$, and μ_4 coordination in [{(dppm)Au$_2$(SnB$_{11}$H$_{11}$)$_2$}$_2$]$^{4-}$.[7] More recently, it was shown that the stannaborate ligand employs η^3(BH) coordination at ruthenium fragments and can behave as an ambident ligand employing both η^3(BH) and η^1(Sn) coordination in ruthenium compounds such as [{(PPh$_3$)$_2$Ru(SnB$_{11}$H$_{11}$)}$_2$].[8] Furthermore, examples have been reported for η^1(Sn) to η^3(BH) rearrangement reactions of the heteroborate, including one example for a reversible η^1(Sn) to η^3(BH) rearrangement between the complexes [Ru(2,7,8-(μ-H)$_3$-*exo*-SnB$_{11}$H$_{11}$)(SnB$_{11}$H$_{11}$)(dppb)]$^{2-}$ and [Ru(SnB$_{11}$H$_{11}$)$_2$(dppb)(MeCN)$_2$]$^{2-}$.[9]

Here we present the synthesis of novel stannaborate iron compounds containing the triphos ligand as well as the synthesis and detailed characterization of bimetallic zwitterionic complexes featuring an ambident stanna-*closo*-dodecaborate ligand. Furthermore, the influence of the *exo*-polyhedral iron fragment on the coordinated stannaborate moiety is discussed.

* To whom correspondence should be addressed. E-mail: lars.wesemann@uni-tuebingen.de.

(1) For recent reviews see: (a) Krossing, I.; Raabe, I. *Angew. Chem.* **2004**, *116*, 2116−2142. (b) Reed, C. A. *Chem. Commun.* **2005**, 1669−1677.

(2) Stasko, D.; Reed, C. A. *J. Am. Chem. Soc.* **2002**, *124*, 1148−1149.

(3) See for example: (a) Teixidor, F.; Barberà, G.; Vaca, A.; Kivekäs, R.; Sillanpää, R.; Oliva, J.; Viñas, C. *J. Am. Chem. Soc.* **2005**, *127*, 10158−10159. (b) McKee, M. L. *Inorg. Chem.* **2002**, *41*, 1299−1305. (c) Zharov, I.; Weng, T. C.; Orendt, A. M.; Barich, D. H.; Penner-Hahn, J.; Grant, D. M.; Havlas, Z.; Michl, J. *J. Am. Chem. Soc.* **2004**, *126*, 12033−12046. (d) Clarke, A. J.; Ingleson, M. J.; Kociok-Köhn, G.; Mahon, M. F.; Patmore, N. J.; Rourke, J. P.; Ruggiero, G. D.; Weller, A. S. *J. Am. Chem. Soc.* **2004**, *126*, 1503−1517. (d) Saxena, A. K.; Maguire, J. A.; Hosmane, N. S. *Chem. Rev.* **1997**, *97*, 2421−2461.

(4) Chapman, R. W.; Kester, J. G.; Folting, K.; Streib, W. E.; Todd, L. J. *Inorg. Chem.* **1992**, *31*, 979−983.

(5) (a) Jutzi, P.; Galow, P.; Abu-Orabi, S.; Arif, A. M.; Cowley, A. H.; Norman, N. C. *Organometallics* **1987**, *6*, 1024−1031. (b) Hosmane, N. S.; de Meester, P.; Maldar, N. N.; Potts, S. B.; Chu, S. S. C.; Herber, R. H. *Organometallics* **1986**, *5*, 772−778. (c) Hosmane, N. S.; Jia, L.; Zhang, H.; Maguire, J. A. *Organometallics* **1994**, *13*, 1411−1423.

(6) Marx, T.; Mosel, B.; Pantenburg, I.; Hagen, S.; Schulze, H.; Wesemann, L. *Chem. Eur. J.* **2003**, *9*, 4472−4478.

(7) (a) Hagen, S.; Pantenburg, I.; Weigend, F.; Wickleder, C.; Wesemann, L. *Angew. Chem.* **2003**, *115*, 1539−1543; *Angew. Chem., Int. Ed.* **2003**, *42*, 1501−1505. (b) Hagen, S.; Wesemann, L.; Pantenburg, I. *Chem. Commun.* **2005**, 1013−1015.

(8) Gädt, T.; Grau, B.; Eichele, K.; Pantenburg, I.; Wesemann, L. *Chem. Eur. J.* **2006**, *12*, 1036−1045.

(9) Gädt, T.; Wesemann, L. *Dalton Trans.* **2006**, 328−329.

10.1021/om060328m CCC: $33.50 © 2006 American Chemical Society
Publication on Web 06/29/2006

Scheme 1. One-Pot Synthesis of [1-{Fe(MeCN)$_2$(triphos)}-SnB$_{11}$H$_{11}$] (1) from FeBr$_2$

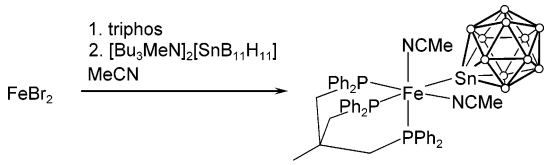

1

Scheme 2. Synthesis of [2,7,8-(μ-H)$_3$-{Fe(triphos)}-SnB$_{11}$H$_{11}$] (2) via an η^1(Sn) to η^3(B−H) Rearrangement

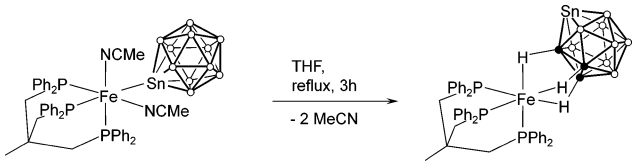

1 2

Results and Discussion

Synthesis. The successful synthesis of the zwitterionic ruthenium stannaborate complex [1-{Ru(MeCN)$_2$(triphos)}-SnB$_{11}$H$_{11}$] motivated us to synthesize the corresponding iron analogue.[10] The reaction is carried out as a one-pot synthesis using FeBr$_2$ as starting material, which is reacted with triphos in acetonitrile. Subsequent addition of an acetonitrile solution of [Bu$_3$MeN]$_2$[SnB$_{11}$H$_{11}$] leads to the formation of a purple precipitate, which can easily be isolated by filtration. The purple zwitterionic compound [1-{Fe(MeCN)$_2$(triphos)}-SnB$_{11}$H$_{11}$] (**1**) is insoluble in common solvents.

A number of examples for η^1(Sn) to η^3(BH) rearrangement reactions under the loss of acetonitrile ligands in ruthenium complexes of stannaborate have recently been described.[9,10] It was thus of interest to find out about the feasibilty of such rearrangements for iron complexes. In fact, the rearrangement proceeds smoothly when a suspension of [1-{Fe(MeCN)$_2$-(triphos)}-SnB$_{11}$H$_{11}$] in THF is heated for 3 h, during which time the purple solid dissolves under the formation of a dark violet solution of [2,7,8-(μ-H)$_3$-{Fe(triphos)}-SnB$_{11}$H$_{11}$] (**2**), which can be isolated by evaporation of the solvent. The obtained violet solid is stable toward air.

Now that we had an air-stable compound at hand that can be prepared on a multigram scale in a convenient way, we were interested in the properties of the stannaborate moiety. The objective was to compare the nucleophilicity of the η^3(B−H−Fe)-coordinated stannaborate with the parent heteroborate [SnB$_{11}$H$_{11}$]$^{2-}$. It is known from Todd's work on the synthesis of [SnB$_{11}$H$_{11}$]$^{2-}$ that the stannaborate behaves as a nucleophile and can easily be methylated at the tin atom at room temperature using MeI.[4] Thus we attempted the methylation of the tin atom of the η^3(B−H−Fe)-coordinated stannaborate using an excess of methyliodide in THF. No reaction occurs at room temperature, as monitored by ^{31}P NMR and ^{11}B NMR spectroscopy.

To probe whether the tin atom would still coordinate to transition metal fragments, we decided to react metal fragments with a labile ligand such as the readily available series of M(CO)$_5$(THF) (M = Cr, Mo, W) with **2**. As monitored by IR spectroscopy, addition of **2** to a freshly prepared THF solution of M(CO)$_5$(THF) (M = Cr, Mo, W) yields the bimetallic complexes [1-{M(CO)$_5$}-2,7,8-(μ-H)$_3$-{Fe(triphos)}-SnB$_{11}$H$_{11}$] (M = Cr, Mo, W) (**3**, **4**, **5**) within minutes. Evaporation of the solvent and subsequent recrystallization from THF/hexane or CH$_2$Cl$_2$/hexane gives dark red crystalline materials in good yields.

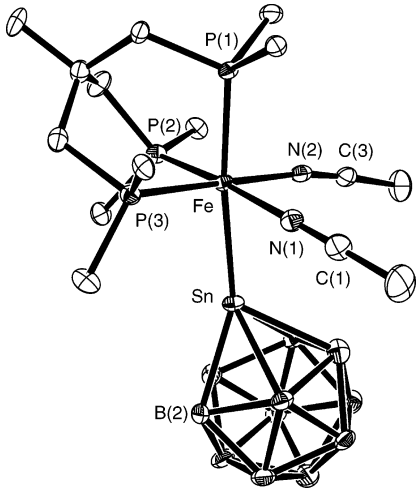

Figure 1. Molecular structure of [1-{Fe(MeCN)$_2$(triphos)}-SnB$_{11}$H$_{11}$], **1**. The hydrogen atoms and the phenyl rings except the *ipso*-carbon atoms have been omitted for clarity. Selected bond distances [Å] and angles [deg]:C(1)−N(1) 1.132(7), C(3)−N(2) 1.134(7), B(2)−Sn 2.310(6), B(3)−Sn 2.327(5), B(4)−Sn 2.329(6), B(5)−Sn 2.343(6), B(6)−Sn 2.329(6), N(1)−Fe 1.953(4), N(2)−Fe 1.942(4), Fe−P(1) 2.264(1), Fe−P(2) 2.249(1), Fe−P(3) 2.276(1), Fe−Sn 2.587(1), N(2)−Fe−N(1) 83.63(17), N(1)−Fe−P(1) 96.96(13), N(1)−Fe−P(2) 171.43(13), N(1)−Fe−P(3) 93.43(13), P(2)−Fe−P(1) 90.26(5), P(2)−Fe−P(3) 91.67(5), P(1)−Fe−P(3) 86.11(5), N(1)−Fe−Sn 80.60(12), N(2)−Fe−Sn 79.85(11), P(1)−Fe−Sn 172.96(5), P(2)−Fe−Sn 91.70(4), P(3)−Fe−Sn 100.59(4).

Solid-State Structure. To elucidate the solid-state structure of the obtained compounds, we carried out single-crystal X-ray diffraction analyses. Carefully layering a solution of FeBr$_2$ and triphos in acetonitrile with an acetonitrile solution of [Bu$_3$MeN]$_2$-[SnB$_{11}$H$_{11}$] leads to the formation of single crystalline material within 2 days. Remarkably, the structure contains four acetonitrile solvent molecules in addition to the two coordinated acetonitrile ligands. The molecular structure of compound [1-{Fe(MeCN)$_2$(triphos)}-SnB$_{11}$H$_{11}$] (**1**) is depicted in Figure 1 together with selected bond lengths and angles. The iron−tin bond length amounts to Fe−Sn 2.587(1) Å, which is within the range of known tin−iron separations of 2.41−2.77 Å[11] and somewhat longer than the Fe−Sn bond in [NBu$_4$][CpFe(CO)$_2$-(SnB$_{11}$H$_{11}$)], with a value of 2.479 Å.[12a] All three phosphorus−iron separations are similar, ranging from Fe−P(2) 2.249(1) Å to Fe−P(3) 2.276(1) Å. Interestingly, the iron−phosphorus bond in *trans* position to the stannaborate ligand of Fe−P(1) 2.264(1) Å is not elongated due to the *trans* influence of the stannaborate ligand as in the corresponding ruthenium complex.[10] The tin−boron distances lie in the range 2.310−2.342 Å, and the average separation is 2.328 Å, which is in accord with previously reported distances ([CpFe(CO)$_2$(SnB$_{11}$H$_{11}$)]$^-$: 2.289−2.342 Å,[12a] [(dppp)Pt(SnB$_{11}$H$_{11}$)$_2$]$^{2-}$: 2.285−2.322 Å,[12b] [Au(SnB$_{11}$H$_{11}$)$_4$]$^{5-}$: 2.293−2.321 Å [6]).

Dark violet crystals suitable for X-ray diffraction analysis of **2** can be grown by layering a dichloromethane solution with hexane. The molecular structure is depicted in Figure 2 and

(10) Gädt, T.; Eichele, K.; Wesemann, L. *Dalton Trans.* **2006**, 2706−2713.

(11) Holt, M.; Wilson, W.; Nelson, J. H. *Chem. Rev.* **1989**, *89*, 11−49.

(12) (a) Wesemann, L.; Marx, T.; Englert, U.; Ruck, M. *Eur. J. Inorg. Chem.* **1999**, 1563−1566. (b) Wesemann, L.; Hagen, S.; Marx, T.; Pantenburg, I.; Nobis, M.; Driessen-Hölscher, B. *Eur. J. Inorg. Chem.* **2002**, 2261−2265.

Scheme 3. The Reduced Nucleophilicity of the η^3(B−H−Fe)-Coordinated Stannaborate Prevents Methylation

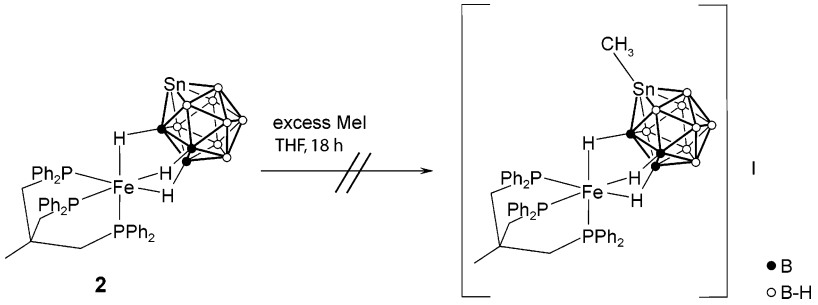

2

Scheme 4. Synthesis of Bimetallic, Zwitterionic Compounds with $[SnB_{11}H_{11}]^{2-}$ as Ambident Ligand

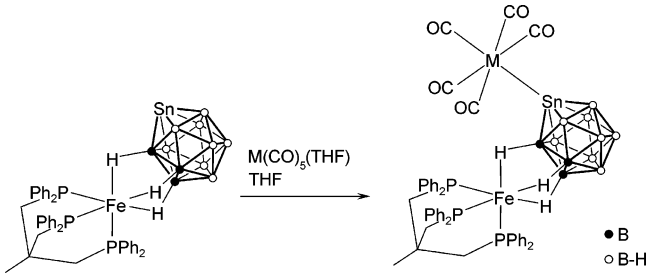

2

3 (M = Cr)
4 (M = Mo)
5 (M = W)

Scheme 5. The Two Isomers of 2 Present in the Solid State with Occupancies of 95.7:4.3 According to the Structure Refinement

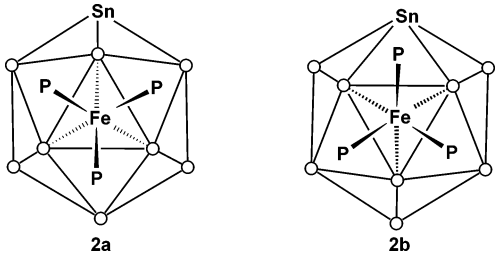

2a **2b**

establishes the η^3(B−H−Fe) coordination of the stannaborate moiety. A special feature of the crystal structure is the disorder of the heteroborate which is coordinated at the iron fragment in two different modes with occupancies of 95.7:4.3. The major isomer employs one B−H vertex from the first B_5-belt and two B−H vertexes from the second B_5-belt for the η^3(B−H−Fe) coordination, while the minor isomer uses two B−H vertexes from the first B_5-belt and one vertex from the second B_5-belt (Scheme 5). Recently reported stannaborate ruthenium compounds exhibit analogous disorder of the heteroborate cluster.[8−10] The three boron−iron separations in the major isomer are similar (B−Fe: 2.227−2.267 Å), which is also true for the iron−phosphorus separations (Figure 2), which are somewhat shorter than in **1**. Compared to **1** the tin−boron distances from the first B_5-belt to the tin atom are elongated and lie in the range 2.360−2.423 Å with an average separation of 2.401 Å, the Sn−B(2) 2.360(3) Å distance being smaller than the other four tin−boron separations from the first B_5-belt.

The molecular structure of [1-{$Cr(CO)_5$}-2,7,8-(μ-H)$_3$-{Fe(triphos)}-$SnB_{11}H_{11}$] (**3**) is depicted in Figure 3, and structural parameters of **3**, **4**, and **5** are given in Table 1. Again, the η^3(B−H−Fe) coordination is clearly established, but there is no disorder of the η^3(B−H−Fe)-coordinated moiety in the crystal structures of **3**, **4**, and **5**. The Fe−B and Fe−P distances are similar for all three compounds and are in the range 2.230−2.309 Å for the Fe−B separations and 2.200−2.238 Å for the Fe−P distances. These values are similar to those of **2** and indicate that the bonding situation around the iron fragment is not affected significantly by the tin coordination. The B(2)−Sn separation is smaller than the other four B(3−6)−Sn separations for all three compounds, and the average distances from the tin atom to the boron atoms of the first B_5-belt are 2.341 Å (**3**), 2.357 Å (**4**), and 2.347 Å (**5**). These values lie between those of the exclusively η^3(B−H−Fe)- and η^1(Sn−Fe)-coordinated stannaborate moieties and thus demonstrate that the cluster geometry is significantly affected by both coordination forms: η^1(Sn) coordination reduces the separation of the tin atom to the first B_5-belt compared to exclusive η^3(B−H) coordination. The metal−tin bond lengths in compounds **3**−**5** are similar to those in the octahedral tin *closo*-clusters $[\{(OC)_5M\}_6Sn_6]^{2-}$.[13] Finally, the carbon metal distances in *trans* position to the stannaborate moiety are slightly smaller than those in *cis* position, as one would expect.

IR Spectroscopy. The infrared spectra of the compounds containing $M(CO)_5$ fragments exhibit the characteristic pattern for pentacarbonyl complexes of approximate C_{4v} symmetry consisting of four bands, namely, $A_1^{(2)}$, B_1, E, and $A_1^{(1)}$. The $A_1^{(1)}$ vibration is mainly localized in the CO ligand in *trans*

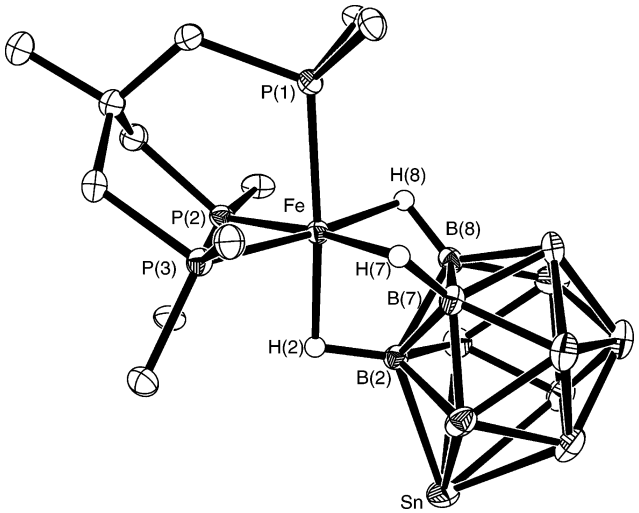

Figure 2. Molecular structure of [2,7,8-(μ-H)$_3$-{Fe(triphos)}-$SnB_{11}H_{11}$], **2**. Only the major isomer is shown. The hydrogen atoms and the phenyl rings except the *ipso*-carbon atoms have been omitted for clarity. Selected bond distances [Å] and angles [deg]: Sn−B(2) 2.360(3), Sn−B(3) 2.419(3), Sn−B(4) 2.400(3), Sn−B(5) 2.403(3), Sn−B(6) 2.423(3), B(2)−Fe 2.267(3), B(7)−Fe 2.271(3), B(8)−Fe 2.237(3), Fe−P(1) 2.219(1), Fe−P(2) 2.200(1), Fe−P(3) 2.220(1), Fe−H(2) 1.79(3), Fe−H(7) 1.80(3), Fe−H(8) 1.78(3), P(2)−Fe−P(1) 90.97(2), P(2)−Fe−P(3) 90.21(2), P(1)−Fe−P(3) 90.73(2), P(1)−Fe−H(2) 174.0(10), P(2)−Fe−H(2) 83.1(10), P(3)−Fe−H(2) 89.1(10).

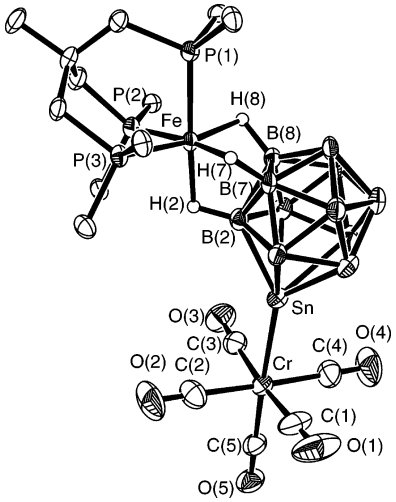

Figure 3. Molecular structure of [1-{$Cr(CO)_5$}-2,7,8-(μ-H)$_3$-{Fe(triphos)}-$SnB_{11}H_{11}$], **3**. The hydrogen atoms and the phenyl rings except the *ipso*-carbon atoms have been omitted for clarity.

Table 1. Structural Parameters of 3, 4, and 5

	3 (M = Cr)	**4** (M = Mo)		**5** (M = W)
M−Sn	2.578(1)	2.735(1)	2.750(1)	2.743(1)
B(2)−Sn	2.286(7)	2.300(6)	2.310(6)	2.296(5)
B(3)−Sn	2.372(7)	2.381(6)	2.357(6)	2.367(6)
B(4)−Sn	2.341(7)	2.369(7)	2.367(6)	2.364(6)
B(5)−Sn	2.355(6)	2.352(6)	2.372(6)	2.353(6)
B(6)−Sn	2.349(7)	2.352(6)	2.381(6)	2.357(6)
C(5)−M	1.843(6)	1.999(7)	1.989(6)	1.984(7)
C(5)−O(5)	1.152(7)	1.144(7)	1.146(7)	1.157(8)
C(1)−M	1.884(8)	2.051(8)	2.007(9)	2.036(7)
C(1)−O(1)	1.136(9)	1.130(9)	1.138(10)	1.145(8)
B(2)−Fe	2.309(7)	2.271(6)	2.292(6)	2.272(5)
B(7)−Fe	2.252(6)	2.246(6)	2.255(6)	2.249(5)
B(8)−Fe	2.230(6)	2.247(6)	2.236(5)	2.260(5)
P(1)−Fe	2.204(2)	2.200(2)	2.202(2)	2.205(1)
P(2)−Fe	2.206(2)	2.219(2)	2.212(1)	2.224(1)
P(3)−Fe	2.238(1)	2.212(2)	2.231(1)	2.216(1)
C(1)−M−Sn	87.5(2)	92.8(2)	93.9(2)	93.8(2)
C(5)−M−Sn	177.3(2)	170.8(2)	171.6(2)	170.4(2)
P(1)−Fe−H(2)	170(2)	171(2)	171(2)	174(2)
P(1)−Fe−H(7)	93(2)	82(2)	95(2)	84(2)
P(1)−Fe−H(8)	81(2)	93(2)	83(2)	96(2)

position to the stannaborate, and it is commonly accepted that the wavenumber of this vibration may serve as a rough gauge of the π-bonding ability of the respective *trans*-standing ligand.[14] The low wavenumbers of the $A_1^{(1)}$ vibrations are similar for **3**, **4**, and **5** (1890−1896 cm^{-1}) and lie below those of stannylene fragments or $SnCl_3$ bonded to $M(CO)_5$.[15,16] They can be compared to the $A_1^{(1)}$ frequencies of pentacarbonyl complexes of amines such as cyclohexylamine,[14b] indicating the weak π-acceptor character of the stannaborate ligand. The broad B−H stretching band is present in the IR spectra of all compounds and is accompanied by the B−H−M band at lower wavenumbers for compounds **2** and **3**, which is masked by the CO bands in compounds **4** and **5**.

NMR Spectroscopy in Solution. The NMR spectroscopic characterization of **1** in solution was hampered by the insolubility of the compound in common solvents. Fortunately, the solubility of the other zwitterionic compounds was large enough to carry out multinuclear NMR measurements in solution. The η^3(B−H−Fe) coordination of the stannaborate moiety of **2** is corroborated by the ^{1}H, ^{11}B, and ^{119}Sn NMR spectra, which closely resemble the respective spectra of the analogous ruthenium complex.[10] All characteric features are present, namely, the occurrence of broad hydridic ^{1}H signals in the ^{1}H{^{11}B} NMR spectrum at −9.8 and −10.3 ppm and the presence of five signals in the ^{11}B NMR spectrum, reflecting the reduced local symmetry, as well as the low-frequency shift of the ^{119}Sn NMR signal, which appears at −623 ppm compared to free stannaborate (−546 ppm). Interestingly, the ^{31}P{^{1}H} NMR spectrum reveals a broad singlet at 54.2 ppm at room temperature, which implies equivalent phosphorus atoms (Figure 4). However, upon cooling, new signals appear, giving rise to an A_2B spin system with a coupling constant of ^2J(P,P) = 55.7 Hz. Since there is no line-broadening involved in the appearance of new signals, one can exclude coalescence, and therefore the singlet at room temperature is not caused by a dynamic process that would render the three phosphorus atoms equivalent but by accidental isochrony.

The pentacarbonyl derivatives exhibit similar ^{1}H, ^{11}B{^{1}H}, and ^{31}P{^{1}H} NMR spectra, which are in close analogy to those of **2**. There is no accidental isochrony present at room temperature in the ^{31}P{^{1}H} NMR spectra, which show signals due to A_2B spin systems around 52.1 and 53.5 ppm with coupling constants of ^2J(P,P) = 56.8 Hz. Thus the ^{1}H, ^{11}B{^{1}H}, and ^{31}P{^{1}H} NMR spectra confirm that the bonding situation around the iron atom remains essentially unchanged. Suitable nuclei to probe the coordination of the tin atom are the ^{119}Sn and ^{13}C nucleus. In fact, the chemical shift of the tin atom is moved to higher frequency compared to **2**, with values of −228 (**3**), −328 (**4**), and −439 ppm (**5**). The shift toward higher frequencies upon coordination of the tin atom is a general trend in the coordination chemistry of $[SnB_{11}H_{11}]^{2-}$.[8,12] Since **3** and **5** are the first stannaborate complexes of chromium and tungsten, a reference value is available only for **4** at the moment, which is the ^{119}Sn chemical shift of $[(C_7H_7)Mo(CO)_2(SnB_{11}H_{11})]^-$ with a resonance at −257 ppm.[12a] Due to the very large line-width ($\nu_{1/2} \approx 400$ Hz) of the ^{119}Sn NMR resonance of **5**, the tungsten−tin coupling constant could not be resolved. The ^{13}C{^{1}H} NMR spectra of the three pentacarbonyl compounds reveal two peaks in the CO region exhibiting tin satellites with *cis* coupling constants of $^2J(^{117/119}Sn,^{13}C)$ = 69 (**3**), 108 (**4**), and 57 Hz (**5**) and a *trans* coupling constant of $^2J(^{117/119}Sn,^{13}C)$ = 80 Hz (**5**). Due to the limited solubility of the zwitterionic compounds, the *trans* $^2J(^{117/119}Sn,^{13}C)$ coupling could not be obtained for **3** and **4**.

Solid-State NMR Spectroscopy. Because of the insolubility of **1**, we decided to carry out solid-state NMR experiments on **1** and the other compounds presented in this study. Phosphorus-31 and tin-119 magic-angle-spinning (MAS) NMR experiments not only provide isotropic chemical shifts that can be compared to chemical shifts obtained from solution NMR but also allow the characterization of the ^{31}P and ^{119}Sn chemical shift tensors via analysis of spinning sideband intensities.[17] In the case of **1**, the crystalline material was dried under reduced pressure. Its ^{31}P variable-amplitude cross-polarization (VACP) MAS NMR spectrum reveals three signals with tin satellites at 48.5, 30.5, and 19.4 ppm. The analogous ruthenium complex also shows three peaks, at 48.7, 22.9, and 5.1 ppm, and we were able to assign the peak at lowest frequency to the phosphorus *trans* to tin because of the large ^2J(Sn,P) coupling constant of 1597 Hz,

(13) (a) Schiemenz, B.; Huttner, G. *Angew. Chem.* **1993**, *105*, 295−296; *Angew. Chem., Int. Ed. Engl.* **1993**, *32*, 297−298. (b) Renner, G.; Kircher, P.; Huttner, G.; Rutsch, P.; Heinze, K. *Eur. J. Inorg. Chem.* **2001**, 973−980.

(14) (a) Cotton, F. A.; Kraihanzel, C. S. *J. Am. Chem. Soc.* **1962**, *84*, 4432−4438. (b) Kraihanzel, C. S.; Cotton, F. A. *Inorg. Chem.* **1963**, *2*, 533−540.

(15) (a) Marks, T. J. *J. Am. Chem. Soc.* **1971**, *93*, 7090−7091. (b) Petz, W. *Chem. Rev.* **1986**, *86*, 1019−1047.

(16) Ruff, J. K. *Inorg. Chem.* **1967**, *6*, 1502−1504.

Table 2. Crystal Data and Structure Refinement Parameters for 1, 2, 3, 4, and 5

	1	2	3	4	5
formula	$C_{53}H_{68}B_{11}FeN_6P_3Sn$	$C_{42}H_{52}B_{11}Cl_2FeP_3Sn$	$C_{54}H_{66}B_{11}CrFeO_7P_3Sn$	$C_{96}H_{108}B_{22}Cl_8Fe_2Mo_2O_{10}P_6Sn_2$	$C_{48}H_{54}B_{11}Cl_4FeO_5P_3SnW$
fw	1175.49	1014.10	1265.43	2670.02	1422.92
cryst syst	orthorhombic	monoclinic	triclinic	monoclinic	monoclinic
space group	$P2_12_12_1$	$P2_1/n$	$P\bar{1}$	$P2_1/a$	$P2_1/n$
a (Å)	16.7406(6)	14.4482(5)	12.0705(9)	23.1640(8)	13.7646(6)
b (Å)	17.8630(5)	19.7150(9)	13.2630(10)	20.2790(9)	20.3159(9)
c (Å)	19.7267(7)	16.8746(7)	21.0976(16)	27.1721(10)	21.7745(11)
α (deg)	90	90	76.283(6)	90	90
β (deg)	90	102.968(3)	77.687(6)	112.210(3)	102.298(4)
γ (deg)	90	90	70.274(6)	90	90
volume (Å^3)	5899.0(3)	4684.1(3)	3055.7(4)	11816.9(8)	5949.3(5)
Z	4	4	2	4	4
D(calc) (g/cm^3)	1.324	1.438	1.375	1.501	1.589
μ (mm^{-1})	0.791	1.091	0.941	1.175	2.889
F(000)	2416	2056	1292	5344	2800
size (mm^3)	0.36 × 0.15 × 0.13	0.26 × 0.24 × 0.20	0.27 × 0.19 × 0.13	0.31 × 0.26 × 0.15	0.29 × 0.17 × 0.14
θ range (deg)	3.19−29.24	3.23−29.29	3.15−29.61	2.95−31.20	3.04−31.19
total no. of reflns	38 597	80 114	35 963	131 701	34 640
no. of unique reflns	15 055 [R(int) = 0.0682]	12 640 (R(int) = 0.0537)	15 920 [R(int) = 0.0805]	35 188 [R(int) = 0.0979]	17 490 [R(int) = 0.0424]
no. of data/restraints/params	15 055/0/679	12 640/0/561	15 920/0/687	35 188/6/1384	17 490/22/697
GOF	1.142	1.100	1.160	1.055	1.052
final R_{ind} [$I>2\sigma(I)$]	R1 = 0.0644, wR2 = 0.1166	R1 = 0.0433, wR2 = 0.1007	R1 = 0.0812, wR2 = 0.1503	R1 = 0.0808, wR2 = 0.1256	R1 = 0.0605, wR2 = 0.1148
residual ρ (e Å^{-3})	1.058 and −1.024	1.984 and −1.756	0.961 and −0.931	1.319 and −0.921	3.751 and −2.054

Table 3. Wavenumbers (cm^{-1}) of Selected Bands

	B−H	CO
1	2468	
2	2497, 2055 (B−H−Fe)	
3	2527, 2080 (B−H−Fe)	2051 ($A_1^{(2)}$), 1977 (B_1), 1932 (E), 1892 ($A_1^{(1)}$)
4	2519	2067 ($A_1^{(2)}$), 1989 (B_1), 1943 (E), 1896 ($A_1^{(1)}$)
5	2529	2066 ($A_1^{(2)}$), 1981 (B_1), 1934 (E), 1890 ($A_1^{(1)}$)

Table 4. ^{31}P MAS NMR Data

	δ_{iso}	δ_{11}	δ_{22}	δ_{33}	Ω^a	κ^b	^2J(Sn,P)
1	48.5	170	45	−69	239	−0.05	693
	30.5	120	26	−55	175	−0.07	561
	19.4	119	10	−71	190	−0.12	415
2	62.1	166	66	−46	211	0.06	
	54.0	141	71	−49	190	0.26	
	48.5	134	57	−45	179	0.13	
3	57.7	164	64	−55	219	0.09	
	43.1	127	57	−53	180	0.22	
4	58.2	162	65	−52	214	0.09	
	43.7	128	58	−54	182	0.23	
5	58.2	163	66	−54	217	0.11	
	43.6	130	55	−53	183	0.18	

[a] Span of the chemical shift tensor, $\Omega = \delta_{11} - \delta_{33}$. [b] Skew of the chemical shift tensor, $\kappa = 3(\delta_{22} - \delta_{iso})/\Omega$.

Table 5. ^{119}Sn MAS NMR Data

	δ_{iso}	δ_{11}	δ_{22}	δ_{33}	Ω^a	κ^b
1	−383	−205	−205	−740	535	1.00
2a	−645	−221	−742	−973	752	−0.39
2b	−617	−201	−689	−962	761	−0.28
3	−208	270	42	−935	1205	0.62
4	−303	137	−132	−915	1052	0.49
5	−411	−23	−294	−917	894	0.39

[a] Span of the chemical shift tensor, $\Omega = \delta_{11} - \delta_{33}$. [b] Skew of the chemical shift tensor, $\kappa = 3(\delta_{22} - \delta_{iso})/\Omega$.

compared to the much smaller 350 Hz for the peak at 48.7 ppm; the satellites for the peak at 22.9 ppm were not resolved.[10] Such an assignment is not possible in the case of **1** because the ^2J(Sn,P) coupling constants are of similar magnitude (Table 4). At present, we cannot rationalize this observation, but given that the M−P distances in **1** are similar (vide supra), in contrast to the ruthenium analogue, it seems another indication that there are distinct electronic differences between the iron and ruthenium complexes. On the other hand, the ^{31}P chemical shift tensors of **1** and the ruthenium analogue are similar. The ^{119}Sn VACP/MAS NMR spectrum of **1** shows a resonance at −383 ppm (Figure 5), which is shifted toward lower frequency compared to [NBu_4][$CpFe(CO)_2(SnB_{11}H_{11})$], with a value of −208 ppm,[12a] and to $Ru(MeCN)_2$(triphos)($SnB_{11}H_{11}$), with −304 ppm.[10] A comparison of the principal components of the ^{119}Sn chemical shift tensor in **1** with the Ru analogue[10] indicates that all three components are shifted by about 100 ppm to lower frequencies in the iron complex.

The ^{31}P VACP/MAS NMR spectrum of **2** shows three peaks that are shifted to higher frequencies by 14−28 ppm compared to **1**, mainly due to changes in δ_{22} and δ_{33} (Table 4). Interestingly, the ^{119}Sn VACP/MAS NMR spectrum of **2** exhibits two sets of signals belonging to isomeric species present

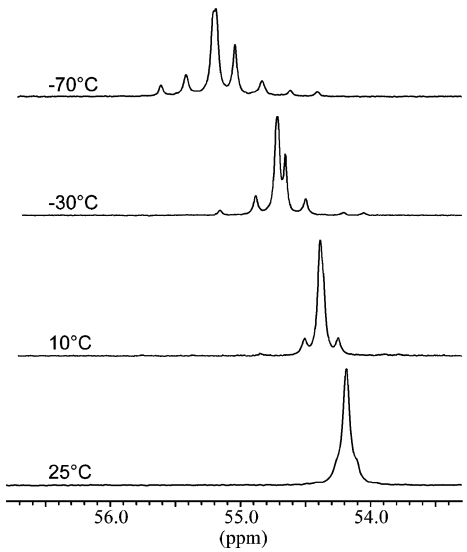

Figure 4. Variable-temperature ^{31}P{^{1}H} NMR measurements of **2** in CD_2Cl_2.

(17) (a) Herzfeld, J.; Berger, A. E. *J. Chem. Phys.* **1980**, *73*, 6021−6030. (b) Maricq, M. M.; Waugh, J. S. *J. Chem. Phys.* **1979**, *70*, 3300−3316.

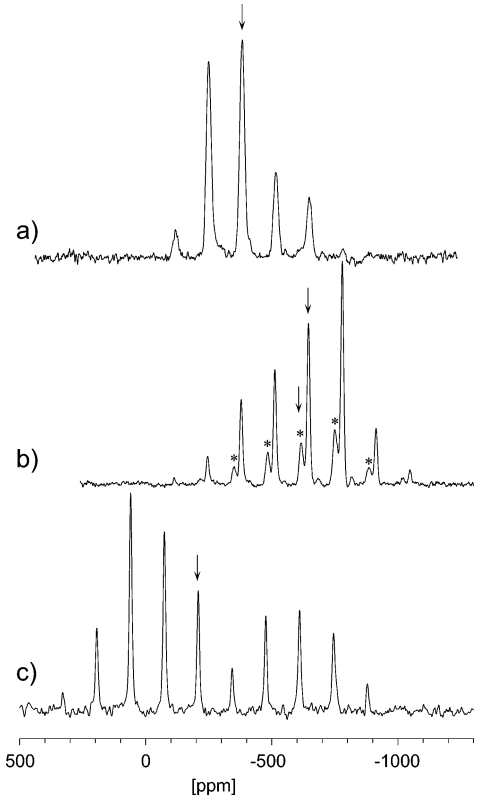

Figure 5. Solid-state ^{119}Sn VACP/MAS NMR spectra obtained at 4.7 T and a spinning rate of 10 kHz; isotropic peaks are indicated by arrows: (a) **1**; (b) **2** (the asterisk denotes signals belonging to the minor isomer); (c) **3**.

in the solid state with a ratio of 68% (**2a**) to 32% (**2b**) (Table 5, Figure 5). The occurrence of two species in the solid-state NMR spectrum is in agreement with the structure refinement of the X-ray diffraction data (Scheme 5). A similar finding has recently been reported for the analogous ruthenium complex.[10] The ^{119}Sn isotropic chemical shifts of −617 and −645 ppm are shifted to lower frequencies, characteristic of a η^3(B−H)-coordinated stannaborate moiety.[8,10]

Although the crystal structures of **3**−**5** do not show molecular symmetry, the ^{31}P VACP/MAS NMR spectra of **3**−**5** reveal two resonances, with the peak around 58 ppm twice as intense as the peak around 43 ppm. The peak at 58 ppm actually shows a spinning-rate-dependent splitting.[18] It is not surprising that the ^{31}P isotropic chemical shifts as well as the respective tensor components are very similar (Table 4). The ^{119}Sn isotropic chemical shifts of **3**−**5** are in good agreement with the chemical shifts in solution (Table 5), and the spectra exhibit only one set of signals, as one would expect for a system without any disorder of the stannaborate cluster. The increasing shift of δ_{iso} to lower frequency by roughly 100 ppm increments on changing the metal from chromium in **3** to molybdenum in **4** to tungsten in **5** is caused by changes in δ_{11} and δ_{22}, while δ_{33} remains relatively invariant. Similar trends are known for the ^{31}P chemical shift tensors of phosphines coordinated to those transition metals[19] and have also been the subject of theoretical studies.[20] As Figure 5 demonstrates, the ^{119}Sn chemical shift tensors appear to be very sensitive to the coordination mode of the stannaborate unit. Exclusive η^1(Sn) coordination as in **1** leads to the lowest span and a positive skew, while exclusive η^3(B−H) coordination as in **2** enlarges the span and, more dramatically, changes the sign of the skew. Simultaneous employment of both coordination modes affords a positive skew and the largest span of the chemical shift tensor.

Conclusions. The η^3(B−H) coordination of a (triphos)Fe^{2+} fragment at the stanna-*closo*-dodecaborate cluster leads to a significant change in the NMR properties and structural parameters of the heteroborate cluster. The iron−stannaborate complex **2** displays a strongly reduced nucleophilicity at the tin atom. Coordination at the tin atom can be achieved by reacting metal fragments with labile ligands, which establishes a general pathway to bimetallic complexes with $[SnB_{11}H_{11}]^{2-}$ as ambident ligand.

Experimental Section

General Procedures. All manipulations were carried out under dry argon in Schlenk glassware. Solvents were dried and purified by standard methods and stored under argon. Elemental analyses were performed by the Institut für Anorganische Chemie Universität Tübingen using a Vario EL analyzer. Chemicals were purchased commercially except $[Bu_3MeN]_2[SnB_{11}H_{11}]$, which was synthesized using a modified protocol of Todd's original work.[4]

NMR. NMR spectra were obtained using a Bruker DRX-250 NMR spectrometer equipped with a 5 mm ATM probe head and operating at 250.13 (^{1}H), 80.25 (^{11}B), 62.90 (^{13}C), 101.25 (^{31}P), and 93.25 MHz (^{119}Sn). Chemical shifts are reported in δ values relative to external TMS (^{1}H, ^{13}C), $BF_3{\cdot}Et_2O$ (^{11}B), 85% aqueous H_3PO_4 (^{31}P), or $SnMe_4$ (^{119}Sn) using the chemical shift of the solvent ^{2}H resonance frequency. Simulations of NMR spectra obtained from solution were done using WINDAISY.[21] NMR spectra of solid samples were obtained on a Bruker DSX-200 NMR spectrometer operating at 200.13 (^{1}H), 81.01 (^{31}P), and 74.60 MHz (^{119}Sn). The powdered samples were spinning about the magic angle at 10 kHz in 4 mm o.d. zirconia rotors. Phosphorus-31 NMR spectra were obtained after variable-amplitude cross-polarization (VACP) from protons and under high-power ^{1}H decoupling. Tin-119 NMR spectra were obtained after single-pulse excitation, or VACP, and under high-power ^{1}H decoupling. Chemical shifts are referenced with respect to external 85% aqueous H_3PO_4 (^{31}P) or $SnMe_4$ (^{119}Sn) using the chemical shift of ammonium dihydrogen phosphate, 0.81 ppm, or $SnCy_4$, −97.35 ppm, as secondary chemical shift reference. MAS spectra were analyzed using the program HBA.[22] Errors in chemical shifts and coupling constants are estimated to be 0.5 ppm and 40 Hz (^{31}P) or 2 ppm and 100 Hz (^{119}Sn), because of the greater line widths in the ^{119}Sn MAS spectra (0.8−1.0 kHz) attributed to ^{119}Sn−^{10,11}B spin−spin interactions. Principal components of the chemical shift tensors are accurate to about 2% of Ω.

Crystallography. X-ray data for compounds **1**−**5** were collected on a Stoe IPDS 2T diffractometer and were corrected for Lorentz and polarization effects and absorption by air. Numerical absorption correction based on crystal-shape optimization was applied for all data. The programs used in this work are Stoe's X-Area[23] and the WinGX suite of programs[24] including SHELXS and SHELXL[25] for structure solution and refinement.

(18) (a) Wu, G.; Wasylishen, R. E. *Inorg. Chem.* **1994**, *33*, 2774−2778. (b) Wu, G.; Eichele, K.; Wasylishen, R. E. In *Phosphorus-31 NMR Spectral Properties in Compound Characterization and Structural Analysis*; Quin, L. D., Verkade, J. G., Eds.; VCH Publishers: New York, 1994; pp 441−450.

(19) (a) Wosnick, J. H.; Morin, F. G.; Gilson, D. F. R. *Can. J. Chem.* **1998**, *76*, 1280−1283. (b) Eichele, K.; Wasylishen, R. E.; Kessler, J. M.; Solujić, L.; Nelson, J. H. *Inorg. Chem.* **1996**, *35*, 3904−3912.

(20) (a) Kaupp, M.; Malkin, V. G.; Malkina, O. L. In *Encyclopedia of Computational Chemistry, Vol. 3*; von Ragué Schleyer, Ed.; John Wiley & Sons: Chichester, 1998; pp 1857−1866. (b) Kaupp, M. *Chem. Ber.* **1996**, *129*, 535−544.

(21) *WinDaisy 4.0*; Bruker Franzen Analytik, 1996.

(22) Eichele, K. *HBA32 1.5.8*; Tübingen, 2005.

(23) *X-AREA 1.26*; Stoe & Cie GmbH: Darmstadt, 2004.

(24) Farrugia, L. J. *J. Appl. Crystallogr.* **1999**, *32*, 837−838.

[1-{Fe(MeCN)$_2$(triphos)}-SnB$_{11}$H$_{11}$]·4MeCN (1). All hydrogen atoms were placed in calculated positions and refined with isotropic thermal parameters. The acetonitrile solvate molecule C18, C19, N6 was refined isotropically.

[2,7,8-(μ-H)$_3$-{Fe(triphos)}-SnB$_{11}$H$_{11}$]·CH$_2$Cl$_2$ (2). All hydrogen atoms except the hydrogen atoms H2, H7, and H8 were placed in calculated positions and refined with isotropic thermal parameters. The B−H−Fe protons H2, H7, and H8 were located on difference maps and allowed to refine freely. The stannaborate moiety displayed disorder over two positions with an occupancy of 95.7:4.3 and was refined by constraining the minor heteroborate icosahedron to a variable-metric rigid group using the AFIX 9 constraint. The boron atoms and the tin atom of the minor isomer were kept isotropic, and the hydrogen atoms were omitted. H3 of the major isomer was also omitted because of its close proximity to the tin atom of the minor heteroborate.

[1-{Cr(CO)$_5$}-2,7,8-(μ-H)$_3$-{Fe(triphos)}-SnB$_{11}$H$_{11}$]·2THF (3). All hydrogen atoms except the hydrogen atoms H2, H7, and H8 were placed in calculated positions and refined with isotropic thermal parameters. H2, H7, and H8 were located on difference maps and allowed to refine freely. The THF solvent carbons atoms C15, C16, C17, and C18 were refined isotropically.

2 [1-{Mo(CO)$_5$}-2,7,8-(μ-H)$_3$-{Fe(triphos)}-SnB$_{11}$H$_{11}$]·4CH$_2$Cl$_2$ (4). There are two independent molecules and four solvent molecules in the asymmetric unit. All hydrogen atoms except the hydrogen atoms H2, H7, and H8 were placed in calculated positions and refined with isotropic thermal parameters. H2, H7, and H8 were located on difference maps and allowed to refine freely. The phenyl ring C29−C34 is disordered over two positions with a ratio of 56.3:43.7, and the disordered atoms were refined isotropically. Two CH_2Cl_2 molecules showed disorder and were refined over two positions with occupancies of 76.5:23.5 and 74.3:25.7. Two DFIX and one DANG restraint were applied for the dichloromethane molecule C89, Cl3, and Cl4. C89 was refined isotropically.

[1-{W(CO)$_5$}-2,7,8-(μ-H)$_3$-{Fe(triphos)}-SnB$_{11}$H$_{11}$]·2CH$_2$Cl$_2$ (5). All hydrogen atoms except the hydrogen atoms H2, H7, and H8 were placed in calculated positions and refined with isotropic thermal parameters. H2, H7, and H8 were located on difference maps and allowed to refine freely. The phenyl ring C29−C34 is disordered over two positions with a ratio of 55.3:44.7, and the disordered atoms were refined isotropically.

Syntheses. [1-{Fe(MeCN)$_2$(triphos)}-SnB$_{11}$H$_{11}$] (1). To a solution of 216 mg (1.00 mmol) of $FeBr_2$ in 20 mL of MeCN was added 625 mg (1.00 mmol) of triphos. After 15 min 650 mg (1 mmol) of [Bu$_3$MeN]$_2$[SnB$_{11}$H$_{11}$] in 20 mL of MeCN was added dropwise via syringe. Immediately the color of the reaction mixture changed from red to violet and a pink precipitate formed. The precipitate was isolated by filtration and washed with MeCN (3 × 5 mL), yielding 627 mg (62%) of a pink solid. Single-crystals suitable for X-ray diffraction analysis were grown by carefully layering the acetonitrile solution of $FeBr_2$ and triphos with an acetonitrile solution of [Bu$_3$MeN]$_2$[SnB$_{11}$H$_{11}$]. IR (KBr): 2468 (s, BH), 2268 (vw, MeCN). Anal. Calcd (%) for $C_{45}H_{56}B_{11}FeN_2P_3Sn$: C, 53.44; H, 5.58; N, 2.77. Found: C, 52.57; H, 4.83; N, 2.72. Repeated elemental analyses of the crystalline material as well as the powder consistently gave rather poor results, which might be caused by the acetonitrile solvent molecules (four solvent molecules are present in the crystal structure) and the lability of the acetonitrile ligands.

[2,7,8-(μ-H)$_3$-{Fe(triphos)}-SnB$_{11}$H$_{11}$] (2). A suspension of 506 mg (0.50 mmol) of **1** in 40 mL of THF was refluxed for 3 h. The solid dissolved and formed a dark violet solution. Afterward the solvent was removed under reduced pressure and the remaining violet powder was recrystallized from CH_2Cl_2/hexane, yielding 441 mg (95%). IR (KBr): 2497 (s, BH), 2055 (w, B−H−Fe). ^{1}H NMR (CD_2Cl_2): δ 6.8−7.2 (m, 30H, C_6H_5), 2.55 (s, 2H, CH_2), 2.45 (s, 4H, CH_2), 1.78 (s, 3H, CH_3), −9.8 (br, 1H, B−*H*−Fe), −10.3 (br, 2H, B−*H*−Fe). ^{11}B NMR (CD_2Cl_2): δ −0.4, −6.1, −7.9, −14.3, −24.7 (3B, ^1J(B,H) = 78.3 Hz, B−*H*−Fe). ^{13}C{^{1}H} NMR (CD_2Cl_2): δ 135.2−136.5 (m, q-aromat. C), 128.3−132.0 (m, aromat. C), 39.2 (m, CH_3), 37.2 (m, q−C), 35.3−35.8 (br m, CH_2). ^{31}P{^{1}H} NMR (CD_2Cl_2, RT): δ 54.2 (s). ^{31}P{^{1}H} NMR (CD_2Cl_2, −70 °C): δ 58.1 (m, 2P, ^2J(P,P) = 55.7 Hz), 57.6 (m, 1P, ^2J(P,P) = 55.7 Hz). ^{119}Sn{^{1}H} NMR (CD_2Cl_2): δ −623. Anal. Calcd (%) for $C_{41}H_{50}B_{11}FeP_3Sn·CH_2Cl_2$: C, 49.74; H, 5.17. Found: C, 49.61; H, 5.02.

[1-{Cr(CO)$_5$}-2,7,8-(μ-H)$_3$-{Fe(triphos)}-SnB$_{11}$H$_{11}$] (3). A solution of 66 mg (0.300 mmol) of $Cr(CO)_6$ in 150 mL of THF was irradiated for 90 min using a medium-pressure Hg-UV lamp. To the resulting yellow solution was added 279 mg (0.300 mmol) of [2,7,8-(μ-H)$_3$-{Fe(triphos)}-SnB$_{11}$H$_{11}$], and stirring was continued for 15 min. The dark red solution was concentrated in vacuo to 30 mL and layered with hexane. Within 2 days dark red crystals of X-ray diffraction quality formed and were collected via filtration. Yield: 283 mg (84%). IR (KBr): 2527 (m, BH), 2080 (w, B−H−Fe), 2051 (s, CO, $A_1^{(2)}$), 1977 (m, CO, B_1), 1932 (vs, CO, E), 1892 (m, CO, $A_1^{(1)}$). ^{1}H{^{11}B} NMR (CD_2Cl_2): δ 6.8−7.2 (m, 30H, C_6H_5), 2.54 (m, 6H, CH_2), 1.82 (s, 3H, CH_3) −9.95 (br, 1 H, B−*H*−Fe), −10.21 (br, 2H, B−*H*−Fe). ^{11}B NMR (CD_2Cl_2): δ −3.7 (br), −9.3 (br), −16.4 (br), −25.7 (2B, ^1J(B,H) = 84.1 Hz, *B*−H−Fe), −28.2 (1B, ^1J(B,H) = 86.1 Hz, *B*−H−Fe). ^{13}C{^{1}H} NMR (d_6-DMSO): δ 211.8 (*trans* CO), 206.6 (*cis* CO, ^2J($^{117/119}$Sn,^{13}C) = 69 Hz) 134.8−136.0 (m, q-aromat. C), 128.6−132.0 (m, aromat. C), 39.2 (m, CH_3), 37.1 (m, q−C), 35.7 (br m, CH_2). ^{31}P{^{1}H} NMR (CD_2Cl_2): δ 53.6 (m, 1P, ^2J(P,P) = 56.8 Hz), 52.1 (m, 2P, ^2J(P,P) = 56.8 Hz). ^{119}Sn{^{1}H} NMR (CD_2Cl_2): δ −228. Anal. Calcd (%) for $C_{46}H_{50}B_{11}CrFeO_5P_3Sn$: C, 49.27; H, 4.49. Found: C, 49.76; H, 4.20.

[1-{Mo(CO)$_5$}-2,7,8-(μ-H)$_3$-{Fe(triphos)}-SnB$_{11}$H$_{11}$] (4). A solution of 79 mg (0.300 mmol) of $Mo(CO)_6$ in 150 mL of THF was irradiated for 90 min using a UV lamp. To the resulting yellow solution was added 279 mg (0.300 mmol) of [2,7,8-(μ-H)$_3$-{Fe(triphos)}-SnB$_{11}$H$_{11}$], and stirring was continued for 15 min. The dark red solution was concentrated in vacuo to 30 mL and layered with hexane. Within 2 days dark red crystals formed and were collected via filtration, yielding 259 mg (74%). Recrystallization from CH_2Cl_2/hexane yielded crystals suitable for X-ray diffraction. IR (KBr): 2519 (m, BH), 2067 (s, CO, $A_1^{(2)}$), 1989 (m, CO, B_1), 1943 (vs, CO, E), 1896 (m, CO, $A_1^{(1)}$). ^{1}H{^{11}B} NMR (CD_2Cl_2): δ 6.9−7.3 (m, 30H, C_6H_5), 2.63 (m, 6H, CH_2), 1.92 (s, 3H, CH_3), −9.82 (br, 1H, B-*H*-Fe), −10.10 (br, 2H, B−*H*−Fe). ^{11}B NMR (CD_2Cl_2): δ −3.2 (br), −8.9 (br), −16.3 (br), −25.6 (2B, ^1J(B,H) = 84.1 Hz, *B*−H−Fe), −27.9 (1B, ^1J(B,H) = 87.1 Hz, *B*−H−Fe). ^{13}C{^{1}H} NMR (d_6-DMSO): δ 212.5 (*trans* CO), 207.4 (*cis* CO, ^2J($^{117/119}$Sn,^{13}C) = 108 Hz), 135.0−136.5 (m, q-aromat. C), 128.3−132.0 (m, aromat. C), 39.4 (m, CH_3), 36.2 (m,q−C), 35.0 (br m, CH_2). ^{31}P{^{1}H} NMR (CD_2Cl_2): δ 53.7 (A_2B, 1P, ^2J(P,P) = 56.7), 52.4 (A_2B, 2P, ^2J(P,P) = 56.7). ^{119}Sn{^{1}H} NMR (CD_2Cl_2): δ −328. Anal. Calcd (%) for $C_{46}H_{50}B_{11}$-$FeMoO_5P_3Sn$: C, 47.42; H, 4.33. Found: C, 47.29; H, 4.55.

[1-{W(CO)$_5$}-2,7,8-(μ-H)$_3$-{Fe(triphos)}-SnB$_{11}$H$_{11}$] (5). A solution of 106 mg (0.300 mmol) of $W(CO)_6$ in 150 mL of THF was irradiated for 90 min using a UV lamp. To the resulting yellow solution was added 279 mg (0.300 mmol) of [2,7,8-(μ-H)$_3$-{Fe(triphos)}-SnB$_{11}$H$_{11}$], and stirring was continued for 15 min. The dark red solution was concentrated in vacuo to 30 mL and layered with hexane. Within 2 days dark red crystals formed and were collected via filtration, yielding 331 mg (88%). Recrystallization from CH_2Cl_2/hexane yielded crystals suitable for X-ray diffraction. IR (KBr): 2529 (m, BH), 2066 (s, CO, $A_1^{(2)}$), 1981

(25) (a) Sheldrick, G. M. *SHELXS-97, Program for the Solution of Crystal Structures*; Göttingen, 1997. (b) Sheldrick, G. M. *SHELXL-97, Program for Crystal Structure Refinement*; Göttingen, 1997.

(m, CO, B_1), 1934 (vs, CO, E), 1890 (m, CO, $A_1^{(1)}$). ^{1}H NMR (CD_2Cl_2): δ 6.82−7.17 (m, 30H, C_6H_5), 2.54 (m, 6H, CH_2), 1.81 (m, 3H, CH_3) −9.94 (br, 1H, B−*H*−Fe), −10.20 (br, 2H, B−*H*−Fe). ^{11}B NMR (CD_2Cl_2): δ −3.5 (br), −9.3 (br), −16.6 (br), −25.8 (2B, ^1J(B,H) = 83.6 Hz, *B*−H−Fe), −28.5 (1B, ^1J(B,H) = 87.5 Hz, *B*−H−Fe). ^{13}C{^{1}H} NMR (d_6-DMSO): δ 203.5 (*trans* CO, $^1J(^{183}W,^{13}C)$ = 169.1 Hz, $^2J(^{117/119}Sn,^{13}C)$ = 80 Hz), 200.3 (*cis* CO, $^1J(^{183}W,^{13}C)$ = 123.9 Hz, $^2J(^{117/119}Sn,^{13}C)$ = 56.8 Hz), 137.9−138.8 (m, q-aromat. C), 131.2−134.6 (m, aromat. C), 42.1 (m, CH_3), 38.8 (m, q−C), 37.5−38.0 (br m, CH_2). ^{31}P{^{1}H} NMR (CD_2Cl_2): δ 53.7 (A_2B, 1P, ^2J(P,P) = 56.9), 52.2 (A_2B, 2P, ^2J(P,P) = 56.9). ^{119}Sn{^{1}H} NMR (CD_2Cl_2): δ −439. Anal. Calcd (%) for $C_{46}H_{50}B_{11}FeO_5P_3SnW$: C, 44.09; H, 4.02. Found: C, 44.15; H, 3.93.

Acknowledgment. Financial support from the Deutsche Forschungsgemeinschaft is gratefully acknowledged.

Supporting Information Available: Full details of crystallographic analyses in CIF format and ORTEP structures of **4** and **5**. This material is available free of charge via the Internet at http://pubs.acs.org.

OM060328M